

Au₃₄⁻: A Chiral Gold Cluster?*

Anne Lechtken, Detlef Schooss,* Jason R. Stairs, Martine N. Blom, Filipp Furche, Nina Morgner, Oleg Kostko, Bernd von Issendorff, and Manfred M. Kappes

Size-selected, ligand-free gold clusters with diameters less than 2 nm can be routinely generated in the gas phase. The pronounced size dependence of their physical and chemical properties is one of their most important features. Surface-deposited gold clusters are particularly interesting for applications in nanotechnology and heterogeneous catalysis.^[1–7] One prerequisite for such applications is a detailed knowledge of the cluster structures.

The extensive literature on theoretical studies of gold clusters has been surveyed in recent reviews.^[8,9] In principle, quantum-chemical methods allow many properties of small gold clusters to be predicted with high accuracy. However, for larger clusters, the large number of possible isomers impedes the search for a global energy minimum. Often, only a small set of the possible structures can be considered, without any guarantee that the global minimum is included in the set. Consequently, progress in the intermediate size regime can only be made through the joint use of experiment and theory.

In this fashion, the structures of small gold cluster anions and cations with up to 13 atoms have been inferred through a comparison of theoretical and experimental collision cross sections from ion-mobility measurements.^[10,11] A remarkable finding in this study was that the 2D → 3D structural transition for Au_n⁻ occurs at the surprisingly large cluster sizes of *n* = 11 and 12. This result was later confirmed through a comparison of photoelectron spectroscopy (PES) data with calculated density of states (DOS) curves.^[12] For Au_n⁻ with *n* = 16–18 and 21–24, experimental and theoretical evidence for hollow

cage-like structures has been reported.^[13–15] Au₂₀⁻ possesses a tetrahedral structure,^[16] which corresponds to a fragment of the face-centered cubic (fcc) structure of bulk gold; the cluster consists only of surface atoms and does not contain any inner atoms.

It has been suggested, on the basis of quantum-chemical calculations, that medium-sized gold clusters, such as Au_n⁻ with *n* = 32–35,^[17,18] 42,^[19] and 50,^[20] also have cage-like structures. In contrast, in a recent study, Au₃₂⁻ was assigned an amorphous, but dense, structure on the basis of a comparison of data from PES and the calculated DOS.^[21] Low-symmetry “disordered” structures have also been proposed by Garzón et al. for Au₂₈ and Au₅₅.^[22] These results were supported by a combined PES and theoretical study by Häkkinen et al., which excluded high-symmetry structures for Au₅₅⁻ (whereas Ag₅₅⁻ and Cu₅₅⁻ have icosahedral structures).^[23]

The PE spectra of several Au_n⁻ clusters, notably for *n* = 14, 20, 34, and 58, show prominent band gaps,^[24] reflecting the large gaps between the highest occupied molecular orbital (HOMO) and the lowest unoccupied molecular orbital (LUMO) in the corresponding neutral clusters. The associated valence-electron counts correlate with the sequence of jellium-shell closings obtained from a simple free-electron model invoking (volume-filling) spherical symmetry. However, beyond the tetrahedral Au₂₀⁻ cluster, it is unclear to what extent larger clusters adopt high-symmetry structures. Determining the structures of these larger clusters is of particular importance for understanding trends in the chemical bonding and growth dynamics of Au_n⁻. Herein, we apply two complementary experimental methods in combination with quantum-chemical calculations to obtain structural information for the previously uncharacterized large-band-gap cluster Au₃₄⁻.

We use a combination of the recently developed trapped-ion electron diffraction (TIED) method,^[25–27] PES, and (time-dependent (TD)) density functional theory (DFT). The TIED technique allows the geometrical structures of cluster ions to be determined. Its potential was recently illustrated by the structure assignments of silver clusters with a wide range of sizes.^[27–29] PES, on the other hand, probes the electronic structure (that is, the DOS), which is strongly influenced by the geometric structure. We compare the experimental DOS to the simulated DOS from TDDFT calculations; such calculations have been successfully applied to the analysis of PE spectra of fullerene dianions.^[30,31] In contrast to PES simulations employing the DOS of the non-interacting Kohn–Sham system, the TDDFT calculations used herein approximate the physical DOS and can properly account for collective effects, such as plasmon excitations. The suitability of TDDFT for the calculation of the excitation energies of

[*] A. Lechtken, Dr. D. Schooss, Dr. J. R. Stairs, Dr. M. N. Blom, Prof. Dr. M. M. Kappes
Institut für Nanotechnologie
Forschungszentrum Karlsruhe
P.O. Box 3640, 76021 Karlsruhe (Germany)
Fax: (+49) 7247-826-368
E-mail: detlef.schooss@int.fzk.de

N. Morgner, O. Kostko, Prof. Dr. B. von Issendorff
Fakultät für Physik
Universität Freiburg
Herman Herderstrasse 3, 79104 Freiburg (Germany)
Priv.-Doz. Dr. F. Furche, Prof. Dr. M. M. Kappes
Institut für Physikalische Chemie
Universität Karlsruhe
Kaiserstrasse 12, 76128 Karlsruhe (Germany)

[**] This research was supported by the Forschungszentrum Karlsruhe and the Deutsche Forschungsgemeinschaft (DFG) through the Center for Functional Nanostructures (CFN) within projects C3.9 and C4.6. J.R.S. acknowledges support from the Alexander von Humboldt Foundation. F.F. thanks R. Ahlrichs for helpful discussions and P. Nava for assistance with the geometry optimizations.



Supporting information for this article is available on the WWW under <http://www.angewandte.org> or from the author.

gold clusters has been established for smaller gold cluster cations^[32] and anions.^[33] The results of our investigations suggest that the Au_{34}^- cluster adopts a chiral structure with C_3 point symmetry. Details of the experimental and TDDFT methods are given in the Supporting Information.

In total, 13 model structures, including different possible structural motifs (for example, icosahedral or close-packed) and morphologies (for example, cage-like or space-filling), were optimized in our DFT calculations. Seven of these model structures are shown in Figure 1. It is apparent that the isomers with the lowest energies, **1–4**, cannot easily be described by the classical structural motifs of icosahedral, decahedral, or close-packed.^[27] However, one common feature of these structures is a four-atom internal tetrahedron that is distorted to varying degrees.

The lowest-energy structure found for Au_{34}^- is chiral with C_3 point symmetry (Table 1). This structure was suggested before by Wales and co-workers^[34,35] as a global minimum for Au_{34} , on the basis of calculations using an empirical Sutton–Chen potential.^[34] It comprises an internal trigonal pyramid (or slightly distorted tetrahedron), of which three faces are covered by a hexagonal arrangement of seven atoms that corresponds to a fragment of a slightly bent Au(111) surface. The base of the internal pyramid is covered by a nearly planar arrangement of six atoms, and the apex is covered by a triangle of three additional atoms that is parallel to the pyramid base. The chirality of the structure is apparent in the helical arrangement of the edge atoms, as shown in the top view of one enantiomer of **1** (Figure 1, right).

Isomer **2**, which has C_{2v} symmetry, is nearly isoenergetic (+0.05 eV) to isomer **1**. This structure was proposed as the ground state of neutral Au_{34} .^[36] It is compact and oblate in shape. Isomers **3** and **4** are 0.17 and 0.42 eV higher in energy, respectively, than the proposed ground state **1**. Isomer **5**, which has D_{3h} symmetry, lies 0.88 eV above the ground state. Unlike isomers **1–4**, it comprises an internal five-atom trigonal bipyramid. The six trigonal faces are each covered by hexagonal arrangements of seven atoms; the capping of each of the two axial atoms of the trigonal bipyramid by four-atom trigonal pyramids leads to a prolate shape. A very similar structure was found as the ground state for Au_{34} in calculations using a Murrell–Mottram potential.^[37] The cage-like isomer **6**, which lies 1.32 eV above the proposed ground state, contains only two internal atoms. The cluster is derived from the hollow icosahedral Au_{32} cluster^[17] by adding two atoms to the central axis of the cage.^[18] As a result of this insertion, the 32-atom icosahedral cage of Au_{34}^- is significantly distorted (symmetry reduction to C_{2h}). Finally, the truncated-tetrahedral isomer **7** was also identified. This cluster is constructed by removing one apex atom from a 35-atom tetrahedron and lies 1.7 eV above the tentative ground state.

Figure 2 shows the experimental reduced molecular scattering functions for the Au_{34}^- cluster and the simulated functions for isomers **1–4** and **6**. A quantitative measure of the agreement between the experimental and theoretical scattering functions is provided by the weighted profile factor R_w (see the Supporting Information).^[27] Of the model structures investigated, the best agreement between the experimental

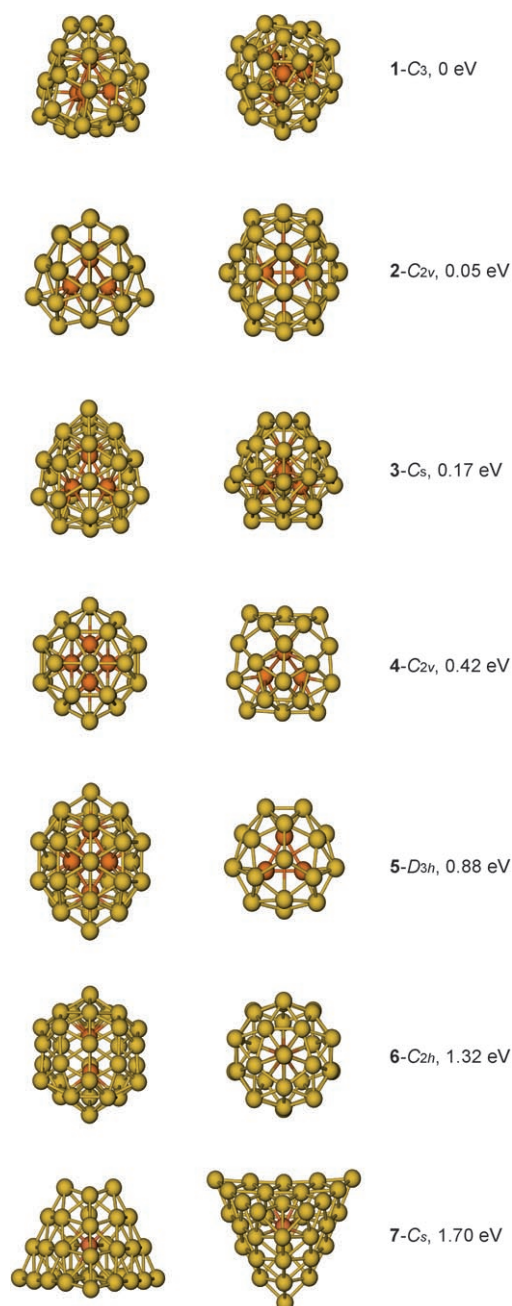


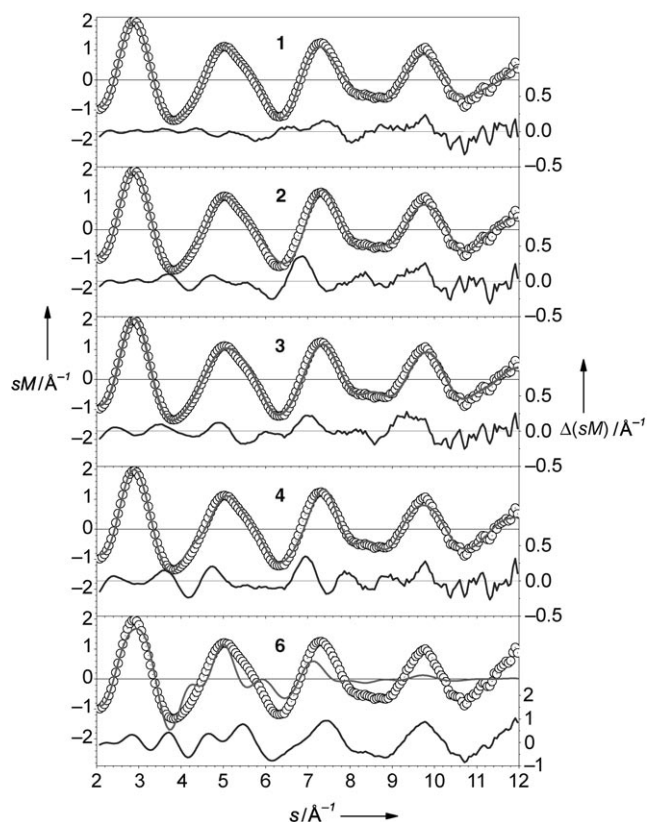
Figure 1. Selected energy-minimum structures found for the Au_{34}^- cluster using DFT calculations. The optimized structures are shown from the side (left) and from the top (right), and their relative stabilities are indicated. The internal atoms are orange.

and theoretical scattering curves is found for the C_3 isomer **1** ($R_w = 3.2\%$; Table 1). Other isomers have significantly higher R_w values, in particular, isomers **4** ($R_w = 9.1\%$) and **5** ($R_w = 19\%$), the cage-like isomer **6** ($R_w = 25\%$), and the truncated-tetrahedral isomer **7** ($R_w = 11\%$). These isomers can in all likelihood be excluded. Although contributions from isomers **2** ($R_w = 5.8\%$) and **3** ($R_w = 6.3\%$) to an isomer mixture cannot be ruled out, the TIED data suggests a dominant contribution from the C_3 isomer **1**. The minor differences between the experimental scattering curve and the curve

Table 1: Properties and R_w values of selected energy-minimum structures for the Au_{34}^- cluster.

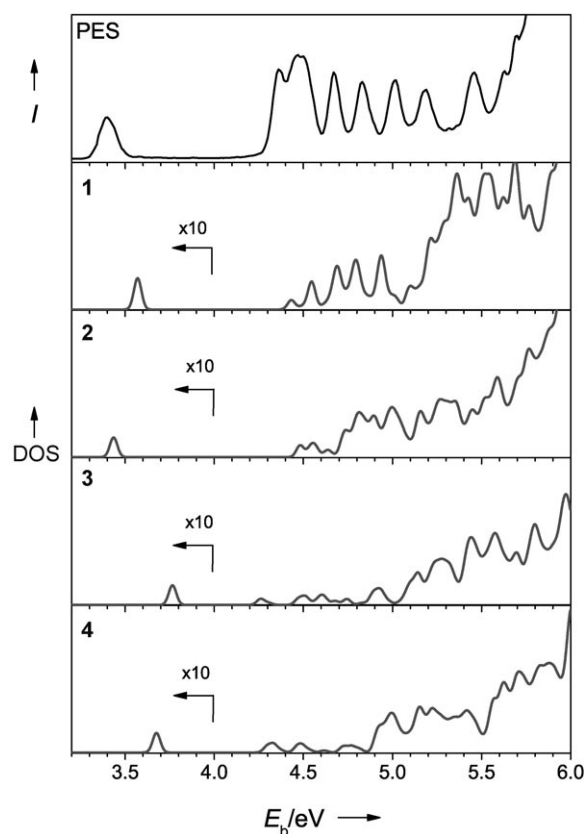
Isomer	$G^{[a]}$	SOMO ^[b]	$\Delta E^{[c]}$ [eV]	$R_w^{[d]}$ [%]
1	C_3	a_1^1	0.00	3.2
2	C_{2v}	b_2^1	0.05	5.8
3	C_s	a_1^1	0.17	6.3
4	C_{2v}	a_1^1	0.42	9.1
5	D_{3h}	$a_2^{\prime\prime 1}$	0.88	19
6	C_{2h}	a_g^1	1.32	25
7	C_s	a_1^1	1.70	11

[a] The point group symmetry. [b] The highest singly occupied molecular orbital. [c] The relative stability with respect to the most stable isomer **1**. [d] The weighted profile factor of the theoretical sM function for the isomer with respect to the experimental TIED sM function for the Au_{34}^- cluster.


Figure 2: Reduced molecular scattering intensities sM for the Au_{34}^- cluster. The upper traces (left axes) show the experimental TIED sM function (\circ) compared to the theoretical sM functions for isomers **1–4** and **6** (—). The lower traces (right axes) show the difference $\Delta(sM)$ functions; note the different scale for isomer **6**.

simulated for isomer **1** are probably caused by the absence of additional vibrational corrections in the present model.

The well-resolved PE spectrum of Au_{34}^- shown in Figure 3, which was recorded at a photon energy of 6.42 eV, is in good agreement with the data reported by Taylor et al.^[24] The spectrum reveals a first peak at 3.4 eV, which corresponds to the vertical detachment energy (VDE), followed by a large energy gap and a series of distinct peaks at higher energies. The gap of 0.96 eV between the first and second excitations


Figure 3: Experimental PES intensity for the Au_{34}^- cluster (top) and calculated TDDFT DOS for isomers **1–4** as a function of the electron binding energy E_b .

can, to a first approximation, be interpreted as the energy difference between the LUMO and the HOMO of the corresponding neutral cluster (at the same geometry as the anion), consistent with an electronic shell closing at 34 s electrons with a $1S^21P^61D^{10}2S^21F^{14}$ angular-momentum configuration.^[38]

To test the model structures further, we compared the DOS simulated for isomers **1–4** using TDDFT calculations to the experimental PE spectrum (Table 2, Figure 3). The isomers excluded by the TIED experiment were not considered. Note that only the experimental electron binding energies and the calculated excitation energies can be compared, because the relative intensities depend on factors not considered in our calculations.

For the C_3 isomer **1**, the VDE is slightly higher (+0.16 eV) than the experimental value, but is still within the range of expected error (± 0.2 eV) of the TDDFT

Table 2: Calculated VDE and band-gap energies (ΔE_{gap}) for isomers **1–4** in comparison to the experimental PES values for the Au_{34}^- cluster.

Isomer	VDE [eV]	ΔE_{gap} [eV]
1	3.56	0.87
2	3.43	1.05
3	3.76	0.50
4	3.67	0.66
PES	3.40	0.96

calculation. Moreover, the band-gap energy and, more importantly, the overall profile of the experimental spectrum agree with the calculated DOS of isomer **1** most closely: it is the only candidate structure that yields a highly modulated DOS curve with a series of nearly equally spaced peaks, as observed in the experimental spectrum. For isomer **2**, the VDE matches the experimental value slightly more closely, but the calculated DOS is only weakly structured. For isomers **3** and **4**, the VDE and the band-gap energy also deviate from the experimental values.

In relating the two types of experimental results, we assume that the cluster ensembles investigated in both experiments were very similar in composition, as they were generated from identical cluster sources under comparable conditions (see the Supporting Information).

The energetic order of the 13 trial structures determined from the DFT calculations, the spectra predicted from the calculations, as well as the comparison of these spectra with the TIED and PES data, suggest that the C_3 isomer **1** is the major contributor to cluster ensemble investigated. An intuitive way to rationalize this structure is to start with a 38-atom truncated octahedron, remove one seven-atom hexagonal plane from the bottom of the truncated octahedron, and then add a triangle on the top, such that an ABAC stacking results. This construction leads to the C_{3v} structure shown in Figure 4, top. The C_{3v} structure is then transformed

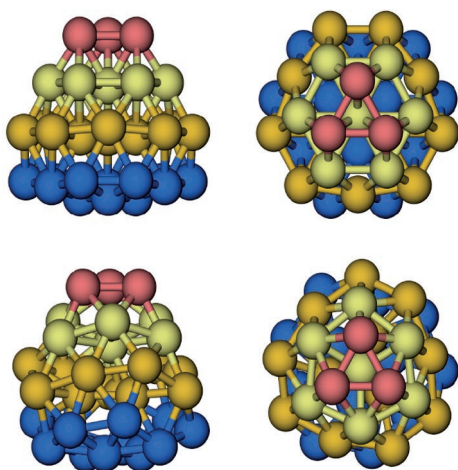


Figure 4. Transformation of the Au_{34}^- modified truncated octahedron with C_{3v} symmetry (top) into isomer **1** with C_3 symmetry (bottom). The different colors are to aid visualization of the transformation.

into the C_3 structure (Figure 4, bottom) by twisting the planes with respect to each other and by repositioning the surface atoms perpendicular to the planes (both steps maintain the C_3 symmetry). This transformation removes the (100) facets of the truncated octahedron and leads to an increased surface density with a higher coordination number.

The optimization of the modified truncated octahedron in C_{3v} symmetry gave an energy of +0.96 eV with respect to that of the C_3 isomer **1**. Since the relative positions of the four internal atoms remain nearly unchanged, this substantial

energy difference is a good approximation to the energy gain upon “reconstruction” of the surface.

Interestingly, a similar structural motif is found in suspended helical multishell gold nanowires:^[39] the planes of nearly hexagonal arrangements of surface atoms are tilted with respect to one another, such that helical strands of surface atoms are formed; this arrangement of surface atoms is similar to that found in isomer **1** of Au_{34}^- .

Furthermore, it is appealing to compare the structure of isomer **1** to the structures of silver clusters, which tend to be icosahedral in this size range.^[28,29] To form a space-filling structure, the interatomic distances in the (111) faces of the icosahedral arrangement must be stretched. But for gold clusters, deviation from the optimal Au–Au bond length involves a large energy penalty, owing to the relativistic contraction of the 6s orbital.^[40,41] Therefore, gold clusters prefer amorphous^[21,22] or cage-like^[16] structures.

Our results reveal another strategy for minimizing the surface energy of a gold cluster, while retaining dense packing and an optimal bond length: surface reconstruction. The investigation of the relevance of this strategy for clusters with other sizes is in progress. Supported gold clusters have recently been shown to be selective oxidation catalysts.^[5,6] On the basis of the chiral cluster proposed herein, enantioselective reactions or asymmetric catalysis should also be considered.

Received: November 23, 2006

Published online: March 9, 2007

Keywords: cluster compounds · density functional calculations · electron diffraction · gold · photoelectron spectroscopy

- [1] W. T. Wallace, R. L. Whetten, *J. Phys. Chem. B* **2000**, *104*, 10964.
- [2] J. Hagen, L. D. Socaciu, M. Eljazyfer, U. Heiz, T. M. Bernhardt, L. Wöste, *Phys. Chem. Chem. Phys.* **2002**, *4*, 1707.
- [3] H. Schwarz, *Angew. Chem.* **2003**, *115*, 4580; *Angew. Chem. Int. Ed.* **2003**, *42*, 4442.
- [4] M. Neumaier, F. Weigend, O. Hampe, M. M. Kappes, *J. Chem. Phys.* **2005**, *122*, 104702.
- [5] A. Sanchez, S. Abbet, U. Heiz, W.-D. Schneider, H. Häkkinen, R. N. Barnett, U. Landman, *J. Phys. Chem. A* **1999**, *103*, 9573.
- [6] S. Lee, C. Fan, T. Wu, S. L. Anderson, *J. Am. Chem. Soc.* **2004**, *126*, 5682.
- [7] P. Schwerdtfeger, *Angew. Chem.* **2003**, *115*, 1936; *Angew. Chem. Int. Ed.* **2003**, *42*, 1892.
- [8] P. Pyykkö, *Angew. Chem.* **2004**, *116*, 4512; *Angew. Chem. Int. Ed.* **2004**, *43*, 4412.
- [9] P. Pyykkö, *Inorg. Chim. Acta* **2005**, *358*, 4113.
- [10] F. Furche, R. Ahlrichs, P. Weis, C. Jacob, S. Gilb, T. Bierweiler, M. M. Kappes, *J. Chem. Phys.* **2002**, *117*, 6982.
- [11] P. Weis, T. Bierweiler, S. Gilb, M. M. Kappes, *Chem. Phys. Lett.* **2002**, *355*, 355.
- [12] H. Häkkinen, B. Yoon, U. Landman, X. Li, H.-J. Zhai, L.-S. Wang, *J. Phys. Chem. A* **2003**, *107*, 6168.
- [13] S. Bulusu, X. Li, L.-S. Wang, X. C. Zeng, *Proc. Natl. Acad. Sci. USA* **2006**, *103*, 8326.
- [14] X. Xing, B. Yoon, U. Landman, J. H. Parks, *Phys. Rev. B* **2006**, *74*, 165423.
- [15] B. Yoon, P. Koskinen, B. Huber, O. Kostko, B. von Issendorff, H. Häkkinen, M. Moseler, U. Landman, *ChemPhysChem* **2007**, *8*, 157.

- [16] J. Li, X. Li, H.-J. Zhai, L.-S. Wang, *Science* **2003**, 299, 864.
- [17] M. P. Johansson, D. Sundholm, J. Vaara, *Angew. Chem.* **2004**, 116, 2732; *Angew. Chem. Int. Ed.* **2004**, 43, 2678.
- [18] X. Gu, M. Ji, S. H. Wei, X. G. Gong, *Phys. Rev. B* **2004**, 70, 205401.
- [19] Y. Gao, X. C. Zeng, *J. Am. Chem. Soc.* **2005**, 127, 3698.
- [20] P. Acioli, J. Jellinek, *Phys. Rev. Lett.* **2002**, 89, 213402.
- [21] M. Ji, X. Gu, X. Li, X. Gong, J. Li, L.-S. Wang, *Angew. Chem.* **2005**, 117, 7281; *Angew. Chem. Int. Ed.* **2005**, 44, 7119.
- [22] I. L. Garzón, J. A. Reyes-Nava, J. I. Rodríguez-Hernández, I. Sigal, M. R. Beltrán, K. Michaelian, *Phys. Rev. B* **2002**, 66, 073403.
- [23] H. Häkkinen, M. Moseler, O. Kostko, N. Morgner, M. A. Hoffmann, B. von Issendorff, *Phys. Rev. Lett.* **2004**, 93, 093401.
- [24] K. J. Taylor, C. L. Pettiette-Hall, O. Cheshnovsky, R. E. Smalley, *J. Chem. Phys.* **1992**, 96, 3319.
- [25] M. Maier-Borst, D. B. Cameron, M. Rokni, J. H. Parks, *Phys. Rev. A* **1999**, 59, R3162.
- [26] S. Krückeberg, D. Schooss, M. Maier-Borst, J. H. Parks, *Phys. Rev. Lett.* **2000**, 85, 4494.
- [27] D. Schooss, M. N. Blom, J. H. Parks, B. von Issendorff, H. Haberland, M. M. Kappes, *Nano Lett.* **2005**, 5, 1972.
- [28] M. N. Blom, D. Schooss, J. Stairs, M. M. Kappes, *J. Chem. Phys.* **2006**, 124, 244308.
- [29] X. Xing, R. M. Danell, I. L. Garzón, K. Michaelian, M. N. Blom, M. M. Burns, J. H. Parks, *Phys. Rev. B* **2005**, 72, 081405.
- [30] O. T. Ehrler, J. M. Weber, F. Furche, M. M. Kappes, *Phys. Rev. Lett.* **2003**, 91, 113006.
- [31] O. T. Ehrler, F. Furche, J. M. Weber, M. M. Kappes, *J. Chem. Phys.* **2005**, 122, 094321.
- [32] A. Schweizer, J. M. Weber, S. Gilb, H. Schneider, D. Schooss, M. M. Kappes, *J. Chem. Phys.* **2003**, 119, 3699.
- [33] S. Gilb, K. Jacobsen, D. Schooss, F. Furche, R. Ahlrichs, M. M. Kappes, *J. Chem. Phys.* **2004**, 121, 4619.
- [34] J. P. K. Doye, D. J. Wales, *New J. Chem.* **1998**, 22, 733.
- [35] D. J. Wales, J. P. K. Doye, A. Dullweber, M. P. Hodges, F. Y. Naumkin, F. Calvo, J. Hernández-Rojas, T. F. Middleton, The Cambridge Cluster Database, <http://www-wales.ch.cam.ac.uk/CCD.html>.
- [36] B. Soule de Bas, M. J. Ford, M. B. Cortie, *J. Mol. Struct.* **2004**, 686, 193.
- [37] N. T. Wilson, R. L. Johnston, *Eur. Phys. J. D* **2000**, 12, 161.
- [38] W. A. de Heer, *Rev. Mod. Phys.* **1993**, 65, 611.
- [39] Y. Kondo, K. Takayanagi, *Science* **2000**, 289, 606.
- [40] E. Aprà, R. Ferrando, A. Fortunelli, *Phys. Rev. B* **2006**, 73, 205414.
- [41] J. P. K. Doye, D. J. Wales, R. S. Berry, *J. Chem. Phys.* **1995**, 103, 4234.